

Quantum size and shape effects on the excited states of $\text{In}_x\text{Ga}_{1-x}\text{As}$ quantum dots

M. Bissiri, G. Baldassarri Höger von Högersthal, and M. Capizzi

Istituto Nazionale di Fisica della Materia - Dipartimento di Fisica, Università di Roma "La Sapienza," Piazzale Aldo Moro 2, I-00185 Roma, Italy

P. Frigeri and S. Franchi

CNR-MASPEC, Parco delle Scienze 37a, I-43010 Fontanini, Parma, Italy

(Received 12 July 2001; published 10 December 2001)

Resonant photoluminescence and excitation photoluminescence experiments have been carried out at low temperature in a number of (InGa)As/GaAs heterostructures. This has allowed us to investigate the dependence of the excited state energy of self-aggregated quantum dots (QD's) on shape and size. Experimental results are compared with theoretical estimates of the QD density of states, and agreement and discrepancies with different theoretical approaches are highlighted. Finally, present results support recent reports of a strong In interdiffusion.

DOI: 10.1103/PhysRevB.64.245337

PACS number(s): 71.38.-k, 63.20.Kr, 78.66.Fd, 81.15.Hi

I. INTRODUCTION

In recent years, zero-dimensional systems, e.g., quantum dots (QD's), have been the object of intensive studies because of their application in optoelectronic devices. In particular, high gain, high quantum efficiency, and low threshold current density with a weak or zero temperature dependence have been predicted and experimentally observed in diode lasers based on QD's.¹⁻³

Although the ground and excited states of self-aggregated quantum dots have been widely investigated, their complete description has been achieved only in the case of colloidal II-VI and III-V QD's,^{4,5} whose spherical shapes can be estimated easily and included in theoretical calculations. In the case of $\text{In}_x\text{Ga}_{1-x}\text{As}/\text{GaAs}$ self aggregated QD's, lenticular, conical or pyramidal shapes have been reported instead. Moreover, the QD electronic properties depend on the theoretical approach followed and on the details of strain distribution. The effective mass approach⁶⁻⁸ gives a crude estimate of the QD ground state, the eight band $\mathbf{k}\cdot\mathbf{p}$ approach⁹⁻¹¹ and the pseudopotential approach¹²⁻¹⁴ predict, instead, QD excited states characterized by a rich structure and energy levels not equally spaced. In fact, the strong mixing of the valence bands caused by the strain, the ensuing removal of orbital degeneracy, and the breakdown of the selection rules for dipole transitions give rise to a large number of allowed radiative transitions.^{9,12,13} However, only a few lines are predicted to dominate the QD optical spectra.

On the experimental side, an evaluation of the QD density of states (DOS), oscillator strengths, polarization, and optical transition selection rules should be obtained directly by absorption spectroscopy. However, due to the extremely low absorption of thin single QD layers, only few experiments have been carried out by means of either highly sensitive techniques¹⁵ or low temperature calorimetric absorption.¹⁶ The discrete nature of the QD DOS has been supported mainly by photoluminescence (PL) spectra in single QD's, where several sharp lines have been observed and attributed to excitonic or multiexcitonic levels.¹⁶⁻²⁴ This single dot approach lacks statistical relevance and no comparison can be

made between different dots or with theoretical calculations because of the lack of detailed structural information (e.g., the indium distribution in the QD). On the other hand, fluctuations in QD size and/or shape and alloy nonuniformity inhomogeneously broaden PL spectra and hamper the investigation of a large number of QD's at once, as in the case of nonresonant photoluminescence. Furthermore, QD excited states are easily investigated in microphotoluminescence, where high excitation densities are achieved by focusing the laser spot to few microns square,²⁵⁻³⁰ but these spectra may be affected by many-body effects.³⁰

The QD feature most relevant for applications is the electron and hole density of states, which is atomiclike because of a 3D carrier confinement. Single-particle DOS is usually investigated by resonant PL (RPL) and PL excitation (PLE).^{4,28,31-37} Therein, only a sub-ensemble of QD's is excited since the excitation energy is lower than that of the 2D InAs "wetting" layer (WL). At low excitation density, this results in a fluorescence line narrowing of the QD PL band.⁴ However, PL, RPL, and PLE spectra are ruled by photon absorption and carrier relaxation and their interpretation is not straightforward, and sometimes controversial.^{34,35} As an example, the issue of carrier relaxation in a system with an atomiclike DOS, namely, the "phonon bottleneck" issue,³⁸ has been addressed often but never solved fully.^{20,39}

In the present work, a comprehensive study of excited states in $\text{In}_x\text{Ga}_{1-x}\text{As}/\text{GaAs}$ QD's is performed by RPL and PLE. Fourteen samples grown by different techniques, with different indium content, and whose average QD ground state emission spans a wide range of energies (from 1.07 to 1.31 eV) were investigated. RPL and PLE techniques are shortly compared in Sec. II, where the equivalence of these two techniques is pointed out. Then, PLE and RPL spectra are presented in Sec. III, where the following results have been achieved. In all samples investigated, a discrete number of well defined resonances is observed in PLE and RPL spectra. The energy of these resonances relative to that of the QD ground state varies sizably from sample to sample. Moreover, in the same sample it changes with detection energy E_{det} in PLE or excitation energy E_{exc} in RPL. For samples

TABLE I. Specifications for the $\text{In}_x\text{Ga}_{1-x}\text{As}/\text{GaAs}$ heterostructures studied in the present work. Samples of the series Rxx have been grown by MOCVD with $x=0.5$, other samples have been grown by MBE with $x=1$. L is the nominal $\text{In}_x\text{Ga}_{1-x}\text{As}$ coverage in monolayers (relative uncertainty $\pm 5\%$), E_{NPL} and Γ are the emission energy and the full width at half maximum, respectively, of the QD band as measured in nonresonant photoluminescence at $T=10$ K. All samples are capped with a 50 nm thick GaAs layer. Samples are listed for decreasing values of E_{NPL} .

Sample	L	E_{NPL}	Γ
	(ML)	(eV)	(meV)
881	1.5	1.310	35
882	1.7	1.290	33
883	1.9	1.280	30
884	2.1	1.266	31
904	1.9	1.265	50
885	2.5	1.230	36
886	3.2	1.220	40
905	2.1	1.200	50
906	2.5	1.140	45
R08	6.0	1.120	50
R19	6.0	1.115	55
R10	6.0	1.115	50
R11	8.0	1.105	50
R05	4.0	1.075	40

with increasing values of the main PL-band peak energy, excited state energies initially increase with respect to the ground state energies, as reported in Ref. 35 where QD's emitting below 1.2 eV were investigated, then saturate, and finally decrease when approaching the energy of the two dimensional InAs layer. These results (i) demonstrate that PLE and RPL resonances are directly related to QD excited state transitions rather than to multiphonon processes; (ii) provide evidence of a combined role of quantum size and quantum shape effects in determining the energy of QD excited states, which are in good agreement with theoretical estimates; (iii) identify two groups of low energy resonances, which are attributed to single phonon replica and transitions involving hole excited states (or local modes); (iv) indicate the absence of a sizable phonon bottleneck; (v) support recent suggestions of a deviation of the effective indium concentration from its nominal value because of a strong In and Ga interdiffusion.^{40,41} Conclusions are drawn in Sec. IV.

II. SAMPLES AND EXPERIMENTAL DETAILS

Nonresonant and resonant PL as well as PLE measurements have been performed on fourteen $\text{In}_x\text{Ga}_{1-x}\text{As}/\text{GaAs}$ samples; see Table I. Nine InAs/GaAs samples of series 8XX and 9YY have been grown by molecular beam epitaxy (MBE) at $T=500\text{--}520^\circ\text{C}$, five $\text{In}_{0.5}\text{Ga}_{0.5}\text{As}$ samples of the series RZZ have been grown by metal-organic chemical vapor deposition (MOCVD) at a temperature varying between 520°C (No. R05) and 580°C (No. R11). The peak energy

of the main band observed in nonresonant PL, E_{NPL} , covers an energy range (1.075 to 1.310 eV; see Table I) wider than in Ref. 35. In all samples non-resonant PL spectra exhibit Gaussian or almost Gaussian bands, thus suggesting a single distribution of QD sizes and shapes. QD's should have the shape of full pyramids with (113) or (114) lateral surfaces in samples of the series 8XX and with (110) lateral surfaces in samples of the series 9YY, as discussed in Ref. 42. Finally, QD's should be shaped as truncated pyramids with (110) lateral surfaces in samples of the series RZZ.⁴³ Unless otherwise specified, optical measurements were carried out at $T=10$ K in a closed cycle, liquid He optical cryostat. A Ti-sapphire tunable laser, used as light source for RPL and PLE, has provided excitation energies varying continuously from about 1.2 to 1.6 eV. A Nd-Yag laser ($E_{\text{exc}}=1.165$ eV) has been used in the energy region below 1.2 eV. Nonresonant PL was performed by means of an Ar^+ laser ($E_{\text{exc}}=2.41$ eV) or a Ti-sapphire laser ($E_{\text{exc}}\geq 1.519$ eV). Low excitation densities ($P\sim 0.5$ W/cm²) have been used, with a laser spot size of the order of 200 μm . The signal was spectrally analyzed by a double 3/8 or a single 1 m monochromator (resolution ≈ 1 meV) and measured by a GaAs photomultiplier, an InGaAs detector, or a N_2 cooled Ge detector. All spectra were corrected for the spectral response of the optical system.

III. EXPERIMENTAL RESULTS

A. Equivalence of RPL and PLE

In this section, the equivalence of PLE and RPL will be shown and the advantages of these techniques with respect to conventional nonresonant PL, NPL, will be pointed out. In NPL, carriers photogenerated in the continuum of the 2D (InGa)As WL (or in the 3D GaAs barrier) are captured by individual QD's and relax to the QD ground state before recombining radiatively. This process gives rise to PL lines whose homogeneous broadening is of the order of tens of μeV .²⁷ Nevertheless, full width at half maximum (FWHM) of NPL bands is of the order of 30–50 meV, see Table I, since QD size and shape have a random distribution.

The above inhomogeneous broadening is reduced when the excitation energy is lower than the WL band gap, as in PLE and RPL.⁴ PLE measurements are made by monitoring the emission energy of QD's whose ground state energy $E_{\text{g.s.}}$ coincides with the detection energy, E_{det} , while E_{exc} spans the QD density of states. A typical PLE spectrum is shown in Fig. 1 (top) for sample 905 ($E_{\text{det}}=1.200$ eV, roughly the peak energy of the NPL spectrum shown in the same figure by a dashed line). For $E_{\text{exc}}\geq 1.4$ eV, the signal is strong and related to absorption in the continuum of states of the WL [heavy-hole (HH) and light-hole (LH) excitonic absorption]. A resonance due to the absorption at the energy of the GaAs free exciton is also resolved ($E_{\text{FE}}=1.515$ eV). Other four peaks appear below the WL continuum, at 1.258, 1.281, 1.313, 1.351 eV (i.e., 58, 81, 113, 151 meV above E_{det} , respectively). These PL peaks are related to the combined effects of absorption and relaxation processes in QD's. For each E_{det} , the PLE signal is given by

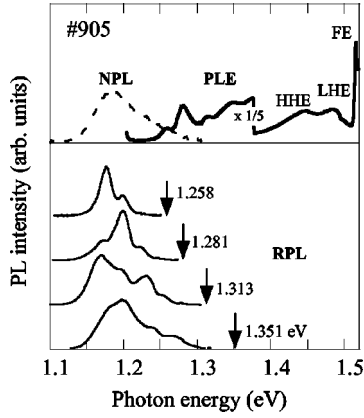


FIG. 1. NPL and PLE (top), and RPL (bottom) spectra in sample No. 905 ($x=1, L=2.1$ ML). The NPL spectrum is shown by a dashed line. The PLE spectrum, taken for $E_{\text{det}}=1.2$ eV, is shown by a solid bold line. The RPL spectra are given for various E_{exc} , which correspond to the peak energies of the main resonances seen in PLE; see vertical arrows.

$$I_{\text{PLE}}(E_{\text{exc}}; E_{\text{det}}) = P_{\text{ab}}(E_{\text{exc}}; E_{\text{det}}) P_{\text{rel}}(E_{\text{exc}} - E_{\text{det}}; E_{\text{det}}) P_{\text{em}}(E_{\text{det}}), \quad (1)$$

where P_{ab} , P_{rel} , P_{em} are the probabilities for the absorption, relaxation, and emission processes, respectively.³⁴ P_{ab} is proportional to the number of QD's with a given excited state energy and a ground state energy $E_{\text{g.s.}} \equiv E_{\text{det}}$, as well as to the oscillator strength for the optical transition from the *system ground state* to the *QD excited state*. P_{rel} is the probability for carrier relaxation from the QD excited state to the QD ground state. At high excitation power, Auger processes^{44,45} or Coulomb scattering with free carriers⁴⁶ dominate carrier relaxation, while at low excitation densities single-phonon or multiphonon processes prevail.^{32,35,45} If P_{rel} is independent of $E_{\text{exc}} - E_{\text{det}}$, PLE fully reproduces optical absorption and the energy spacings between different resonances correspond to differences between QD excited state energies. In the opposite limit for P_{rel} , an accurate determination of the QD DOS is not straightforward, even at low power densities (namely, in absence of Auger processes). In fact, the small window of available longitudinal-optical (LO) phonon energies permits an efficient carrier relaxation from the QD excited state towards the QD ground state only for

$$E_{\text{exc}} \equiv E_i = E_{\text{det}} + nE_{\text{ph}}, \quad (2)$$

where E_i is the energy of the i th QD excited state, E_{ph} is the energy of a LO phonon and n is an integer. Whenever the excitation energy does not satisfy Eq. (2), a “phonon bottleneck” takes place and nonradiative channels dominate carrier relaxation.^{38,47,48} In this case, PLE resonances are equally spaced by multiples of phonon energies and cannot be easily related to QD excited states. It should be noted that PLE spectra exhibit a small broadening (FWHM ~ 15 – 20 meV) because the likely existence of small subensembles of QD's with slightly different excited state energies but same ground state energy. Moreover, multiple scattering with acoustic phonons provides an additional source of broadening.⁴⁹

Similar arguments apply to RPL measurements, which are taken for E_{exc} fixed below the WL band edge energy. Phonon bottleneck effects influence carrier relaxation in the same way as in PLE experiment and resonances are observed for

$$E_{\text{det}} \equiv E_{\text{g.s.}} = E_{\text{exc}} - nE_{\text{ph}}. \quad (3)$$

For E_{exc} in the NPL band, mainly QD ground states are directly excited and the radiative emission is resonant with the laser, except for weak replicas due to exciton-phonon interaction effects.^{36,37} When increasing E_{exc} several resonances due to transitions from QD excited states begin to appear, which coincide with those found in PLE. In all the RPL spectra in the bottom of Fig. 1, a resonance appears at 1.2 eV when E_{exc} coincides with the energy of one of the peaks (1.258, 1.281, 1.313, and 1.351 eV; see arrows in the figure) detected in the PLE spectrum taken for $E_{\text{det}}=1.2$ eV and reported in the top of the figure. Moreover, multiple resonances appear in the RPL spectra whenever E_{exc} corresponds to one of the different resonances of different QD's. As an example, for $E_{\text{exc}}=1.258$ eV one excites the first excited state of a subensemble of QD's emitting at 1.2 eV and the second excited state of a subensemble of QD's emitting at ~ 1.177 eV, namely, ~ 23 meV lower than 1.200 eV. The intensity of each resonance varies with E_{exc} , namely, with the number of QD's excited, as it will be shown in the following. At the same time, a nonresonant band due to carrier absorption in the WL tail continuously grows up for increasing E_{exc} and adds to the resonances due to the QD excited states.²⁸

Notice that a fluorescence narrowing is obtained in RPL as well as in PLE spectra. In fact, the energy dispersion of the QD ground states, as measured by the FWHM in the nonresonant PL, is greater than the energy differences between the resonances observed in RPL or PLE. The residual broadening of RPL spectra can be accounted in the same way as for PLE spectra, except for a reversed role of excited and ground states. Finally, no Stokes shift is observed between the ground and excited state energies estimated by PLE or RPL spectra, as expected on the ground of the discrete QD DOS.

B. RPL and PLE spectra

We will now show PLE and RPL spectra for different QD's in order to establish (i) resonance energies and their dependence on QD size and shape; (ii) QD DOS and/or phonon modes; (iii) evidence, or lack of evidence, of a “phonon bottleneck.” It should be mentioned that, at the low power densities ($P \sim 0.5$ W/cm²) used in present experiments, the line shape of PL bands does not change when P changes by two orders of magnitude and PL intensities scale almost linearly with P . This reasonably excludes that high excitation relaxation mechanisms such as Auger processes contribute to carrier relaxation in the present experiments.⁴⁵

PLE (RPL) spectra are plotted in the top (bottom) of Fig. 2 as a function of relative energy $E_{\text{exc}} - E_{\text{det}}$, for various E_{det} (E_{exc}) and for three different samples. The QD average emission energy, as indicated by the NPL peak energy, E_{NPL} , spans an energy range going from 1.310 eV (No. 881; L

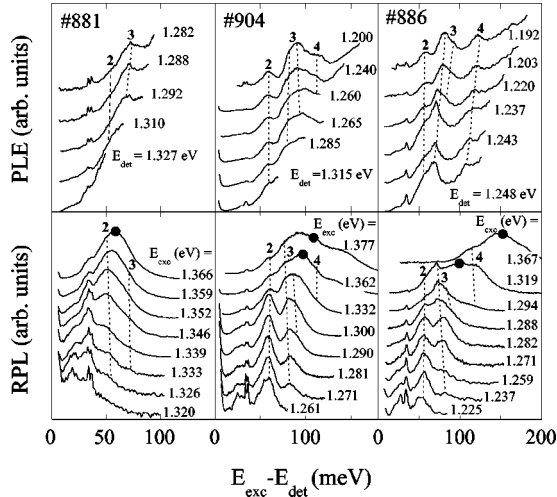


FIG. 2. Top: PLE spectra taken at different values of E_{det} for samples No. 881 ($x=1, L=1.9$ ML), No. 904 ($x=1, L=1.5$ ML), No. 886 ($x=1, L=3.2$ ML). Bottom: RPL spectra for the same samples shown in the top of figure, taken for different E_{exc} . Different resonances in PLE and RPL spectra are labeled by numbers (dashed lines are guides to the eye). Nonresonant contributions to RPL spectra are indicated by dots.

$=1.5$ ML), to 1.265 eV (No. 904; $L=1.9$ ML), to 1.220 eV (No. 886; $L=3.2$ ML). Samples emitting below 1.2 eV, namely, the low-energy limit for emission of the Ti-sapphire laser, will be discussed later.

At a first inspection of PLE spectra, several resonances appear, which are grouped by dashed lines and labeled by numbers. In particular, we list the following.

(i) A resonance E_2 at ~ 50 – 60 meV and a stronger resonance, E_3 , at ~ 70 – 90 meV are well resolved in all samples. Weaker features are also resolved in the energy range of phonon modes. Higher energy and broader resonances are observed in samples with lower E_{NPL} . Similar features can be seen in PLE spectra reported in the literature.^{28,31,34,35}

(ii) Resonance energies vary sensibly from sample to sample as well as in a same sample for different E_{det} . Therefore, the resonance energy depends on the QD ground state energy, $E_{\text{g.s.}}$, selected by the choice of E_{det} , and, consequently, on QD size (and/or shape). As an example, the resonance at $E_2 \sim 55$ meV shifts by about 2 meV when E_{det} spans the QD ground state energy range of each sample (about 40–60 meV, the sample FWHM in NPL spectra). Moreover, E_2 changes by about 6 meV on going from sample 881 to sample 904. Larger shifts are observed in the case of the resonance E_3 at 70 meV, that changes from 70 to 83 meV for a change in E_{det} of 56 meV in sample 886, and changes from 67 to 73 meV in sample 881.

(iii) In most samples, the resonance E_2 is a symmetric singlet. On the contrary, the line shape of E_3 is asymmetric and characterized by shoulders; see, e.g., samples 904 and 886. This indicates a superposition of different optical transitions, whose weight varies with E_{det} and whose energy separation is smaller than the sample inhomogeneous broad-

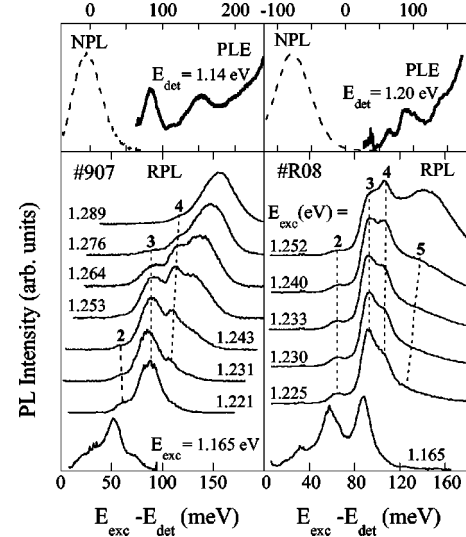


FIG. 3. Left: NPL, PLE, and RPL for sample 907 ($x=1, L=3.1$ ML). Right: NPL, PLE, and RPL for sample R08 ($x=0.5, L=6.0$ ML).

ening. In some cases, as for QD's emitting below ~ 1.15 eV, two or three distinct peaks are sometimes resolved.^{31,34,35}

(iv) A smooth background signal adds to the resonances. Its weight increases with E_{det} and becomes dominant for E_{exc} approaching the energy of the WL band (≈ 1.4 eV). This background is attributed to a partial distribution of carriers in the whole ensemble of QD's because of an absorption in the tail of the WL band due to a continuum of states overlapping the QD excited states.²⁰ Alternatively, such a continuum could be due to direct tunneling between QD's, higher for the excited states.

RPL spectra are shown in the bottom of Fig. 2 vs $E_{\text{exc}} - E_{\text{det}}$ for an easy comparison with PLE spectra. The same resonances observed in PLE are seen in RPL spectra. However, resonances in the energy range of phonon modes are better resolved by RPL at low E_{exc} ; see, e.g., the two Raman peaks due to scattering of the GaAs transverse optical (TO) and LO phonons. An additional resonance is also observed in all samples at ~ 20 – 25 meV. Higher excited states, instead, are less resolved in RPL spectra, where the nonresonant band (centered at E_{NPL} and indicated by full dots in the figure) grows up for increasing E_{exc} until it dominates the spectra for E_{exc} approaching the WL energy.²⁸ This band is the RPL counterpart of the background signal observed in PLE.

RPL spectra of samples emitting below 1.2 eV have been measured by using also a Nd-YAG laser ($E_{\text{exc}}=1.165$ eV) in order to add a spectrum for E_{exc} lower than typical energies of the Ti-sapphire laser. Two typical cases are shown in the bottom of Fig. 3 for an InAs sample grown by MBE (No. 907, left) and an $\text{In}_{0.5}\text{Ga}_{0.5}\text{As}$ sample grown by MOCVD (No. R08, right). RPL intensity is plotted vs $E_{\text{exc}} - E_{\text{det}}$, as in Fig. 2. Nonresonant PL and partial PLE spectra (only the high energy range is covered by the laser) are shown in the top of the figure for the same two samples reported in the bottom. In these samples, the energy spacing between resonances is smaller for QD's emitting below 1.2 eV; see, e.g.,

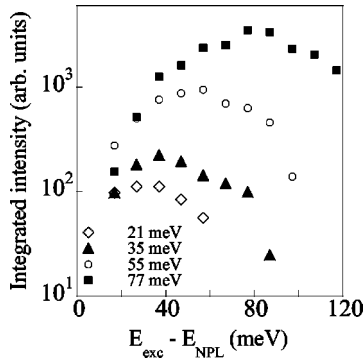


FIG. 4. Strengths of the four Gaussian functions used to fit RPL spectra taken in sample 886 for different E_{exc} as a function of $E_{\text{exc}} - E_{\text{NPL}}$.

resonances for $E_{\text{exc}} = 1.165$ eV and $E_{\text{exc}} \geq 1.2$ eV, and the discussion of the following Fig. 5.

IV. DISCUSSION AND CONCLUSION

Let us now discuss PLE and RPL results. In principle, resonances in these spectra could be related to multiphonon processes. The energy of these phonons ranges³¹ from 29.6 to 36.6 meV in (InGa)As heterostructures and do not change from sample to sample. Therefore, only excited states whose energy differs from that of the QD ground state by multiples of a phonon energy can efficiently relax to the system ground state and give rise to intense PL bands. Resonances, therefore, should be observed only in well defined energy windows, independently of sample as well as of excitation or detection energy. On the contrary, as already observed in the case of the spectra reported in Fig. 2 (and confirmed in the following for all samples; see Fig. 5), the energy of resonances in PLE and RPL spectra *sizably varies* with E_{det} and E_{exc} , respectively, and *is not related to any multiple of phonon energies*. As an example, the energy of E_2 (from 50 to 60 meV) differs from any single phonon energy and is only seldom equal to multiples of a phonon energy. Moreover, when a magnetic field is applied to the system, energy levels of QD's vary sensibly because of the diamagnetic shift and exhibit a Zeeman splitting.⁵⁰ In these experiments, therefore, the energy spacing between different QD states changes and is rarely equal to a multiple of the LO-phonon energy. Nevertheless, strong resonances continue to be observed at all values of magnetic fields.⁵⁰ For these reasons, we attribute RPL and PLE resonances to excited state transitions instead that to multiphonon processes, contrary to what claimed in previous works.^{28,31–35} This attribution permits to obtain a quite precise picture of the QD DOS that agrees very well with recent theoretical models. Moreover, it shows how the energy of these excited states depend on QD shape and size.

The above picture is well supported by the analysis of the RPL spectra of sample 886 shown in Fig. 4. RPL spectra taken for different E_{exc} , as those reported in the bottom of Fig. 2, have been deconvoluted in terms of five Gaussian contributions from electronic states or phonon modes. For simplicity, the five Gaussian peak energies have been kept fixed with E_{exc} (at 21, 35, 55, and 77 meV above the QD

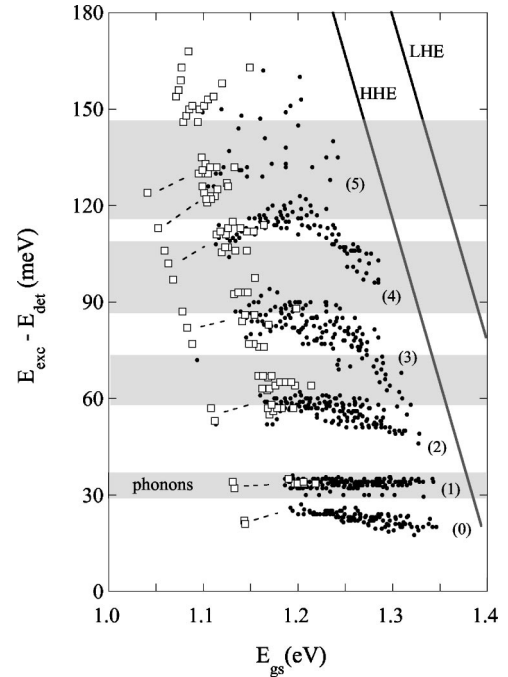


FIG. 5. Resonance energies for all investigated samples, as determined by PLE and RPL spectra at different excitation and detection energies, are reported as a function of the QD ground state energy $E_{\text{g.s.}}$. Labels (n) refer to different clusters of data for QD excited states. Isolated points on the left are data taken by means of Nd-YAG laser. Open squares refer to $\text{In}_{0.5}\text{Ga}_{0.5}\text{As}$ QD's, full dots to InAs QD's. Energy regions that correspond to multiples of phonon energies in (InGa)As/GaAs heterostructures are highlighted in gray.

ground state). NPL contribution has not been included in the fits and the Gaussian full widths at half maximum have been taken of the order of 15–20 meV. The fitted strength of each Gaussian has been reported in the figure as a function of the energy difference $E_{\text{exc}} - E_{\text{NPL}}$. As previously suggested,²⁸ the intensity of each Gaussian exhibits a well defined maximum for $E_{\text{exc}} - E_{\text{NPL}}$ equal to the difference between the energy of the QD excited state and that of the QD ground state.

The values of $E_{\text{exc}} - E_{\text{det}}$ were determined for all sample resonances by PLE at different E_{det} and by RPL at different E_{exc} . They are reported in Fig. 5 as a function of the QD ground state energy $E_{\text{g.s.}}$ that coincides with E_{det} in PLE spectra. In the case of RPL spectra, $E_{\text{g.s.}}$ coincides with the absolute energy of the different resonances, as discussed in Sec. III. Isolated points on the left side are data obtained by means of a Nd-YAG laser in samples such as those investigated in Ref. 35 ($E_{\text{g.s.}} \leq 1.2$ eV). Open squares refer to $\text{In}_{0.5}\text{Ga}_{0.5}\text{As}$ QD's, full dots to InAs QD's. We report also the average values for WL heavy-hole (HHE) and light-hole (LHE) transition energies, whose dependence on InAs coverage has been investigated in a previous work.⁵¹ The fourteen investigated samples largely differ for InAs coverage L and In concentration x ; see Table I. Nevertheless, the energies of the different resonances group into a finite number of “clusters” of data labeled from (0) to (5) in the figure.

These clusters correspond either to well defined sets of QD excited states or to phonon modes. Cluster (2) is associated to an excited state 50–60 meV above the ground state

energy, with an energy spread due to residual fluctuations in QD size and shape rather than to the experimental uncertainty. Cluster (3) ranges from 60 to 90 meV. A complex internal structure makes more difficult a precise estimate of the average peak energy of this cluster. Cluster (4) has a 10 meV energy spread around 110 meV. Data appear scattered at higher energies, see cluster (5), since the inhomogeneous broadening affects more the highest excited states. Finally, two sets of resonances are observed below 50 meV. Cluster (1) collects resonances ranging from 28 to 36 meV, two or three of which ($\sim 28, 33,$ and 35 meV) are often observed in a same sample. Since these resonances are almost independent on $E_{g.s.}$, they are attributed to electron-phonon interaction effects.^{36,37,52} The assignment of the resonances in cluster (0), whose energy decreases for increasing $E_{g.s.}$, is less straightforward. A study of the intensity of these resonances as a function of E_{det} (in PLE) or E_{exc} (in RPL) like that reported in Fig. 4 indicates that these resonances are related likely to hole excited states of the QD's, as suggested also in Ref. 37.

We compare now our results with theoretical estimates of the energy and strength of QD excited states. The agreement with theoretical predictions based on the eight band $\mathbf{k}\cdot\mathbf{p}$ (Refs. 9,35) or the pseudopotential approaches^{13,14} is good. This supports the existence of a finite number of electron bound states as well as the removal of the orbital degeneracy of the bound states with an ensuing richness of transitions between the QD valence and conduction bands. A closer comparison between the theoretical predictions obtained in large QD's emitting at low energy (~ 1 eV) and the corresponding experimental results discloses, however, some differences.

For what concerns the pseudopotential approach, estimates of the QD ground and excited states have been made in the case of QD's with basis 11.3 nm, height 5.6 nm, emitting at 0.959 eV.¹⁴ In this framework, cluster (0) should be due to transitions from the s -like electron state to excited hole states. Clusters (3) and (4) should correspond, instead, to transitions from the ground hole state to the excited, splitted electron p states. Cluster (5) may correspond to transitions from the splitted, first hole-excited states to the electron p states. No transition is predicted, instead, for energy corresponding to that of cluster (2), which may involve higher energy hole-excited states

In the eight band $\mathbf{k}\cdot\mathbf{p}$ method, estimates⁹ have been obtained for the excited states of QD's with basis 17 nm and aspect ratio 0.5 emitting at 1.025 eV. These estimates are in good agreement³⁵ with experimental results for QD's emitting below 1.2 eV. Within the eight band $\mathbf{k}\cdot\mathbf{p}$ approach, we may classify all transitions observed here, including those in cluster (2). As done in Ref. 35, we will label excitonic transitions toward the ground state by the dominating single particle contribution $|e_{nmp}\rangle|h_{nmp}\rangle$. The first ket refers to an electron state and the second ket indicates a hole state. The first sizable transition involving a hole state is the transition from the $|000\rangle|020\rangle$ state, at about 20 meV. This transition can be related with the weak, low energy resonances observed in our samples around this energy and grouped in cluster (0). A second transition involving a hole state, the

$|000\rangle|210\rangle$, is predicted at 45 meV. This and the first weak resonance involving an electron state, the $|100\rangle|010\rangle$ at ~ 65 meV, may account for cluster (2) at about 50 meV. The $|010\rangle|010\rangle$ and $|100\rangle|110\rangle$ transitions are among the strongest transitions, are almost degenerate, and fall in a region going from 80 to 95 meV. They can be related to cluster (3), which is the strongest in all samples and spans the energy region from 70 to 90 meV. It may be worth noticing here that the splitting in the E_3 manifold coincides with the energy of the first hole-excited state, as measured by E_0 . A weaker resonance $|010\rangle|110\rangle$, predicted at 105 meV, could be assigned to resonance E_4 at about 100 meV. Resonances of cluster (1) have already been attributed to phonon sidebands.^{36,37}

As shown in Fig. 5, present results extend the dependence of the excited state energy on QD size, reported in Ref. 35 for a QD emitting at 1.025 eV, to QD's with different sizes *and shapes* emitting at higher energy. Although the agreement with theoretical predictions of Ref. 35 is rather good, present results indicate that quantum size effects determine excited state energies only for weak carrier confinement and suggest that some other stronger effect should occur for $E_{g.s.} \geq 1.2$ eV. The increase of the excited state energies with $E_{g.s.}$, shown in Fig. 5 for QD ground state energy smaller than 1.2 eV, can be explained, indeed, in terms of *quantum size effects* (the larger $E_{g.s.}$, the smaller the QD size, the larger the energy separation between electronic levels).³⁵ However, E_2 slightly decreases for increasing $E_{g.s.}$ in the whole range above 1.2 eV and only data taken by means of Nd-Yag in QD's emitting below 1.2 eV suggest a reverse trend. In a similar way, E_3 is roughly constant or slightly increases with increasing $E_{g.s.}$ for QD's emitting around 1.2 eV, but it decreases for higher $E_{g.s.}$ values. These two opposite regimes with $E_{g.s.}$ are better seen in the case of cluster (4), which shows a clear maximum for $E_{g.s.}=1.25$ eV, namely, in the range covered by the Ti-sapphire laser. In the same way, the energy difference between contiguous excited states decreases for $E_{g.s.} \geq 1.2$ eV. This behavior, opposite to what expected on the basis of quantum size effects, can be ascribed to *quantum shape effects*. The evolution of the QD DOS for QD with same base b but different height h , namely, for QD with different aspect ratio, $\gamma=h/b$, has been investigated in Ref. 12. Therein, it has been shown that the energy spacing between excited states decreases for decreasing γ , in good agreement with our experimental results. In our samples, indeed, QD emission energies range from 1.07 to 1.31 eV and γ decreases with increasing $E_{g.s.}$; see Sec. II and Ref. 42. Therefore, the dependence of the DOS on QD shape may mask quantum size effects in QD emitting above 1.25 eV, namely, where carrier confinement is weaker.

Recently, it has been reported that the transitions from the ground states of (InGa)As/GaAs QD's with different nominal In concentrations ($x=0.5$ and $x=1.0$) almost coincide both in peak energy and line shape.⁴¹ This has been attributed to strong deviations of the effective In concentrations from their nominal values. These conclusions, supported by x-ray fine structure measurements,⁴¹ are consistent with those drawn on the grounds of tomographic nanometer-scale images of self-assembled InAs/GaAs quantum dots obtained from surface

sensitive x-ray diffraction.⁴⁰ Strong In and Ga intermixing is confirmed here, where we show that the same $x=0.5$ and $x=1.0$ samples investigated in Ref. 41 have also excited state energies at the same energy distance from the ground state; see Fig. 5.

Finally, data reported in Fig. 5 suggest that the phonon bottleneck does not affect present RPL and PLE spectra. In Fig. 5, we have highlighted in gray the energy windows that coincide with multiples of a phonon energy, as determined from resonances in cluster (1) (phonon energy broadening has been included). Most of the resonances fall out of the gray regions, the only regions where efficient multiphonon relaxation should take place in presence of a strong phonon bottleneck. The high optical efficiency of QD samples and the very short rise times in PL signal measured in time resolved experiments⁵³ seem also to exclude important phonon bottleneck effects. On the other hand, the mechanism preventing phonon bottleneck in these zero-dimensional systems has not been identified yet. In fact, fast relaxation by Auger effect or by scattering with free carriers is unlikely at the low power densities of the present experiments. Tentatively, an enhanced coupling with acoustic phonons has been suggested to enlarge the window of phonon energies avail-

able to the system. This process may be induced by the localization of QD wave functions, which results in a mixing of \mathbf{k} bulk states and couples more easily with acoustic phonons at the Brillouin-zone border.⁴⁵ Alternatively, it has been suggested that the coupling with acoustic modes due to LO phonon anharmonicity produces relaxation times only weakly longer than those related to relaxation via LO-phonons.⁴⁹ In this framework, we suggest that localized modes may provide an additional path for carrier relaxation.²⁰ Localized as well as acoustic modes may also warrant hole relaxation from excited states whose energy is lower than LO-phonon energies. However, at this stage, nothing more can be said about these local modes whose signature in resonant spectra should coincide with that of hole excited states E_0 .

ACKNOWLEDGMENTS

It is a pleasure to acknowledge M. Colocci for fruitful discussions and the technical assistance of A. Miriametro and L. Ruggieri. This work has been partially supported by the Project MADESS II.

-
- ¹N. N. Ledentsov, M. Grundmann, D. Bimberg, V. M. Ustinov, S. S. Ruvimov, M. V. Maximov, P. S. Kop'ev, Zh. I. Alferov, U. Richter, P. Werner, U. Gösele, and J. Heydenreich, *Electron. Lett.* **30**, 1416 (1994).
- ²R. L. Sellin, Ch. Ribbat, M. Grundmann, N. N. Ledentsov, and D. Bimberg, *Appl. Phys. Lett.* **78**, 1207 (2001).
- ³Y. Arakawa and H. Sakaki, *Appl. Phys. Lett.* **40**, 939 (1982).
- ⁴D. J. Norris and M. G. Bawendi, *Phys. Rev. B* **53**, 16 338 (1996).
- ⁵U. Banin, C. J. Lee, A. A. Guzelian, A. V. Kadavanich, A. P. Alivisatos, W. Jaskolki, G. W. Bryant, Al. L. Efros, and M. Rosen, *J. Chem. Phys.* **109**, 2306 (1998).
- ⁶M. Grundmann, O. Stier, and D. Bimberg, *Phys. Rev. B* **52**, 11 969 (1995).
- ⁷J.-Y. Marzin and G. Bastard, *Solid State Commun.* **92**, 437 (1994); J.-Y. Marzin, J.-M. Gerard, A. Izrael, D. Barrier, and G. Bastard, *Phys. Rev. Lett.* **73**, 716 (1994).
- ⁸M. A. Cusack, P. R. Briddon, and M. Jaros, *Phys. Rev. B* **56**, 4047 (1997).
- ⁹O. Stier, M. Grundmann, and D. Bimberg, *Phys. Rev. B* **59**, 5688 (1999).
- ¹⁰H. Jiang and J. Singh, *Phys. Rev. B* **56**, 4696 (1997).
- ¹¹Craig Pryor, *Phys. Rev. B* **57**, 7190 (1998).
- ¹²J. Kim, L. W. Wang, and A. Zunger, *Phys. Rev. B* **57**, R9408 (1998).
- ¹³L. W. Wang, J. Kim, and A. Zunger, *Phys. Rev. B* **59**, 5678 (1999).
- ¹⁴L. W. Wang, A. J. Williamson, A. Zunger, H. Jiang, and J. Singh, *Appl. Phys. Lett.* **76**, 339 (2000).
- ¹⁵R. J. Warburton, C. S. Durr, K. Karrai, J. P. Kotthaus, G. Medeiros-Ribeiro, and P. M. Petroff, *Phys. Rev. Lett.* **79**, 5282 (1997).
- ¹⁶M. Grundmann, J. Christen, N. N. Ledentsov, J. Böhrer, D. Bimberg, S. S. Ruvimov, P. Werner, U. Richter, U. Gösele, J. Heydenreich, V. M. Ustinov, A. Yu. Egorov, A. E. Zhukov, P. S. Kop'ev, and Zh. I. Alferov, *Phys. Rev. Lett.* **74**, 4043 (1995).
- ¹⁷D. Hessman, P. Castrillo, M. E. Pistol, C. Pryor, and L. Samuelson, *Appl. Phys. Lett.* **69**, 749 (1996). See also for a review on local photoluminescence techniques: A. Gustafsson, M. E. Pistol, L. Montelius, and L. Samuelson, *J. Appl. Phys.* **84**, 1715 (1998).
- ¹⁸M. Notomi, T. Furuta, H. Kamada, J. Temmyo, and T. Tamamura, *Phys. Rev. B* **53**, 15 743 (1996).
- ¹⁹P. Hawrylak, G. A. Narvaez, M. Bayer, and A. Forchel, *Phys. Rev. Lett.* **85**, 389 (2000).
- ²⁰Y. Toda, O. Moriwaki, M. Nishioka, and Y. Arakawa, *Phys. Rev. Lett.* **82**, 4114 (1999); Y. Toda, T. Sugimoto, M. Nishioka, and Y. Arakawa, *Appl. Phys. Lett.* **76**, 3887 (2000).
- ²¹H. An and J. Motohisa, *Appl. Phys. Lett.* **77**, 385 (2000).
- ²²F. Findeis, A. Zrenner, G. Böhm, and G. Abstreiter, *Phys. Rev. B* **61**, R10 579 (2000).
- ²³J. J. Finley, A. D. Ashmore, A. Lemaître, D. J. Mowbray, M. S. Skolnick, I. E. Itskevich, P. A. Maksym, M. Hopkinson, and T. F. Krauss, *Phys. Rev. B* **63**, 073307 (2001).
- ²⁴A. Lemaître, A. D. Ashmore, J. J. Finley, D. J. Mowbray, M. S. Skolnick, M. Hopkinson, and T. F. Krauss, *Phys. Rev. B* **63**, 161309 (2001).
- ²⁵H. Lipsanen, M. Sopanen, and J. Ahopelto, *Phys. Rev. B* **51**, 13 868 (1995).
- ²⁶S. Raymond, S. Fafard, P. J. Poole, A. Wojs, P. Hawrylak, S. Charbonneau, D. Leonard, R. Leon, P. M. Petroff, and J. L. Merz, *Phys. Rev. B* **54**, 11 548 (1996).
- ²⁷J.-Y. Marzin, J.-M. Gérard, A. Izraël, D. Barrier, and G. Bastard, *Phys. Rev. Lett.* **73**, 716 (1994).
- ²⁸M. J. Steer, D. J. Mowbray, W. R. Tribe, M. S. Skolnick, M. D.

- Sturge, M. Hopkinson, A. G. Cullis, C. R. Whitehouse, and R. Murray, *Phys. Rev. B* **54**, 17 738 (1996).
- ²⁹E. Itskevich, M. S. Skolnick, D. J. Mowbray, I. A. Trojan, S. G. Lyapin, L. R. Wilson, M. J. Steer, M. Hopkinson, L. Eaves, and P. C. Main, *Phys. Rev. B* **60**, R2185 (1999).
- ³⁰R. Heitz, F. Gruffarth, I. Mukhametzanov, M. Grundmann, A. Madhukar, and D. Bimberg, *Phys. Rev. B* **62**, 16 881 (2000).
- ³¹R. Heitz, M. Grundmann, N. N. Ledentsov, L. Eckey, M. Veit, D. Bimberg, V. M. Ustinov, A. Yu. Egorov, A. E. Zhukov, P. S. Kop'ev, and Zh. I. Alferov, *Appl. Phys. Lett.* **68**, 361 (1996).
- ³²K. H. Schmidt, G. Medeiros-Ribeiro, M. Oestereich, P. M. Petroff, and G. H. Döhler, *Phys. Rev. B* **54**, 11 346 (1996).
- ³³F. Adler, M. Geiger, A. Bauknecht, D. Haase, P. Ernst, A. Dörnen, F. Scholz, and H. Schweizer, *J. Appl. Phys.* **84**, 4356 (1997).
- ³⁴R. Heitz, M. Veit, N. N. Ledentsov, A. Hoffmann, D. Bimberg, V. M. Ustinov, P. S. Kop'ev, and Zh. I. Alferov, *Phys. Rev. B* **56**, 10 435 (1997).
- ³⁵R. Heitz, I. Mukhametzanov, O. Stier, A. Madhukar, and D. Bimberg, *Phys. Rev. B* **62**, 11 017 (2000).
- ³⁶M. Bissiri, G. Baldassarri Höger von Högersthal, A. S. Bhatti, M. Capizzi, A. Frova, P. Frigeri, and S. Franchi, *Phys. Rev. B* **62**, 4642 (2000); M. Bissiri, G. Baldassarri Höger von Högersthal, M. Capizzi, V. M. Fomin, V. N. Gladilin, and J. T. Devreese, *Phys. Status Solidi B* **62**, 4642 (2001).
- ³⁷R. Heitz, I. Mukhametzanov, O. Stier, A. Madhukar, and D. Bimberg, *Phys. Rev. Lett.* **83**, 4654 (1999); R. Heitz, H. Born, A. Hoffmann, D. Bimberg, I. Mukhametzanov, and A. Madhukar, *Appl. Phys. Lett.* **77**, 3746 (2000).
- ³⁸H. Benisty, C. M. Sotomayor-Torres, and C. Weisbuch, *Phys. Rev. B* **44**, 10 945 (1991).
- ³⁹J. Urayama, T. B. Norris, J. Singh, and P. Bhattacharya, *Phys. Rev. Lett.* **86**, 4930 (2001).
- ⁴⁰I. Kegel, T.H. Metzger, A. Lorke, J. Peisl, J. Stangl, G. Bauer, J.M. Garcia, and P.M. Petroff, *Phys. Rev. Lett.* **85**, 1694 (2000); I. Kegel, T.H. Metzger, A. Lorke, J. Peisl, J. Stangl, G. Bauer, K. Nordlund, W.V. Schoenfeld, and P.M. Petroff, *Phys. Rev. B* **63**, 035318 (2001).
- ⁴¹M. Galluppi, A. Frova, M. Capizzi, F. Boscherini, P. Frigeri, S. Franchi, and A. Passaseo, *Appl. Phys. Lett.* **78**, 3121 (2001).
- ⁴²M. Grassi Alessi, M. Capizzi, A. S. Bhatti, A. Frova, F. Martelli, P. Frigeri, A. Bosacchi, and S. Franchi, *Phys. Rev. B* **59**, 7620 (1999).
- ⁴³J. Shumway, A. J. Williamson, A. Zunger, A. Passaseo, M. De Giorgi, R. Cingolani, M. Catalano, and P. Crozier (unpublished).
- ⁴⁴R. Ferreira and G. Bastard, *Appl. Phys. Lett.* **74**, 2818 (1999).
- ⁴⁵I. V. Ignatiev, I. E. Kozin, V. G. Davydov, S. V. Nair, J-S. Lee, H-W. Ren, S. Sugou, and Y. Masumoto, *Phys. Rev. B* **63**, 075316 (2001).
- ⁴⁶U. Bockelmann and T. Egeler, *Phys. Rev. B* **46**, 15 574 (1992).
- ⁴⁷T. Inoshita and H. Sakaki, *Phys. Rev. B* **46**, 7260 (1992).
- ⁴⁸K. Mukai, N. Ohtsuka, H. Shoji, and M. Sugawara, *Phys. Rev. B* **54**, R5243 (1996).
- ⁴⁹X. Q. Li, H. Nakayama, and Y. Arakawa, *Phys. Rev. B* **59**, 5069 (1999).
- ⁵⁰L. R. Wilson, D. J. Mowbray, M. S. Skolnick, M. Morifuji, M. J. Steer, I. A. Larkin, and M. Hopkinson, *Phys. Rev. B* **57**, R2073 (1998).
- ⁵¹A. S. Bhatti, M. Grassi Alessi, M. Capizzi, P. Frigeri, A. Bosacchi, and S. Franchi, *Phys. Rev. B* **60**, 2592 (1999).
- ⁵²V. M. Fomin, V. N. Gladilin, J. T. Devreese, E. P. Pokatilov, S. N. Balaban, and S. N. Klimin, *Phys. Rev. B* **57**, 2415 (1998).
- ⁵³B. Ohnesorge, M. Albrecht, J. Oshinowo, A. Forchel, and Y. Arakawa, *Phys. Rev. B* **54**, 11 532 (1996).